

# LOW THERMAL EMITTANCE MEASUREMENTS AT THE PSI-XFEL LOW EMITTANCE GUN TEST FACILITY

Y. Kim\*, A. Andersson, M. Dach, R. Ganter, T. Garvey, C. Gough, C. H. Hauri, R. Ischebeck  
F. Le Pimpec, M. Paraliiev, M. Pedrozzi, T. Schietinger, V. Schlott, B. Steffen, and A. F. Wrulich  
Paul Scherrer Institut, CH-5232 Villigen PSI, Switzerland

## Abstract

To check the performance of a planned low emittance gun for the PSI-XFEL project, a 500 kV pulsed diode based gun test facility was constructed at PSI in 2007. The gun was specially designed to have an adjustable gap between the cathode and the anode, and to allow extensive high gradient tests. Since the electron temperature at the cathode determines the minimum achievable slice emittance, we concentrated our efforts on measuring the thermal emittance of a diamond turned copper cathode. After minimizing emittance contributions from nonlinear electromagnetic RF fields, linear and nonlinear space charge forces, chromatic effects, and image noise in the emittance measurement method, we obtained a small thermal emittance of about  $0.2 \mu\text{m}$  with the copper cathode for the rms laser beam spotsize on the photo-cathode of about  $330 \mu\text{m}$  at 40 MV/m. In this paper, we report on our low thermal emittance measurement results with a diamond turned copper cathode at the LEG facility.

## INTRODUCTION

Since 2003, the Paul Scherrer Institut (PSI) has been investigating the PSI-XFEL facility to supply coherent, ultra-bright, and ultra-short XFEL photon beams covering the wavelengths from 1 Å to 10 nm [1]. To saturate the power of the XFEL photon beams with 60 m long undulators and to build the whole facility within about 800 m, the PSI-XFEL project will use two advanced new technologies; the high voltage pulser based Low Emittance Gun (LEG) and the Cryo In-Vacuum Undulator (CIVU) with a small gap of about 5 mm and a short period of about 15 mm. Additionally, the High-order Harmonic Generation (HHG) based seeded High-Gain Harmonic Generation (HG) scheme will be used to generate spatially as well as temporally coherent soft X-rays covering 1 nm to 10 nm [1–3]. To realize such an advanced and compact PSI-XFEL facility, high quality electron beams with a slice emittance of about  $0.2 \mu\text{m}$ , an rms slice energy spread of 600 keV, and a peak current of 1.5 kA should be transferred to three FEL undulators. Generally, the performance and length of an XFEL facility is mainly determined by the slice emittance and the peak current. The gun is the most critical component which determines the slice emittance at the undulators while the bunch compressor is the key component which supplies the required peak current. Therefore, a 500 kV

pulsed advanced LEG test facility was constructed at PSI in 2007 to study and to optimize the generation of high brightness electron beams [4, 5]. Additionally, a 250 MeV injector test facility will be constructed at PSI by 2009 to study advanced beam diagnostics and advanced injector technologies including low emittance beam transport and bunch length compression [2]. The target beam parameters at the LEG are  $I_{\text{peak}} = 5.5 \text{ A}$ ,  $Q = 0.2 \text{ nC}$  and a slice emittance lower than  $0.2 \mu\text{m}$ . Detailed information on the pulser, diagnostic system, first experimental results, and recent progress of the high gradient tests with various cathode materials at the LEG test facility can be found in references [4–7]. In this paper, we report on our recent low thermal emittance measurement results with a copper cathode at the LEG test facility.

## THE LEG TEST FACILITY

The LEG test facility consists of a 500 kV pulser and a diagnostic beamline with an emittance monitor [4–6]. The high voltage pulser can deliver a stable pulse with a length of 250 ns (FWHM) for a maximum amplitude of 500 kV [4]. For the measurements reported here, the electron beams are generated by sending an UV laser beam on the cathode surface as shown in Fig. 1. The laser consists of a quadrupled Nd:Vanadate (Nd:VAN) passively mode locked picosecond system, and the laser pulse is synchronized with the high voltage pulser to generate an electron bunch at the maximum gradient. Its longitudinal pulse profile is Gaussian with an rms pulse length of 6.5 ps and wavelength of 266 nm. During the normal operation, the laser beam energy is about  $4 \mu\text{J}$  at the last entrance viewport before the cathode. However, to obtain a low bunch charge of about 0.6 pC during the thermal emittance measurements, the laser beam energy at the viewport was reduced down to about  $0.47 \mu\text{J}$  by inserting attenuation filters in the laser transfer beamline. As shown in Fig. 2, the laser transverse profile is also Gaussian with the rms laser beam spotsize of about  $330 \mu\text{m}$ . The laser spotsize can be adjusted with a telescope in the laser transfer beamline.

As shown in Fig. 1, the diagnostic beamline includes five solenoid magnets, an emittance monitor (e-meter), two YAG screens to acquire electron beam images, a wall current monitor to measure electron beam charge nondestructively, and a coaxial Faraday cup with a bandwidth wider than 4 GHz. To allow operation of the LEG test facility with various bunch charges, beam energies, gradients, gap sizes, laser pulse lengths, laser spotsizes, and cathodes, five

\* Mail : Yujong.Kim@PSI.ch

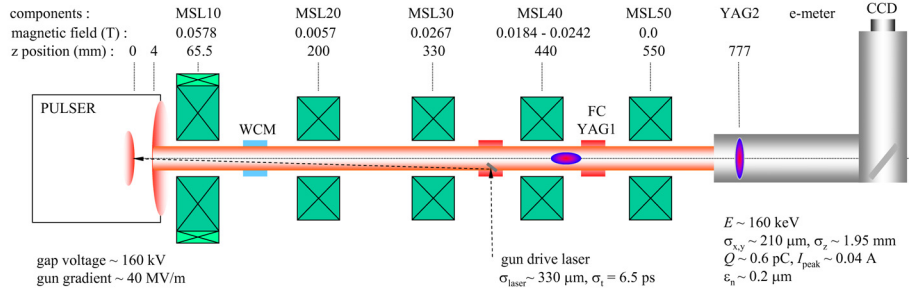


Figure 1: Beamline layout for the thermal emittance measurements with a copper cathode. Here MSL10 to MSL50 are solenoids, and WCM and FC mean a wall current monitor and a Faraday cup. YAG1 and YAG2 are Al-coated YAG:Ce screens.

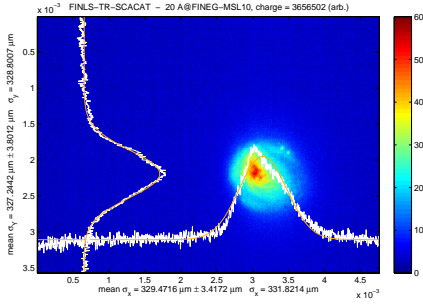


Figure 2: Laser transverse beam profile during thermal emittance measurements. Here  $\sigma_{\text{laser}} \simeq 330 \mu\text{m}$ .

Table 1: Parameters for thermal emittance measurements.

Parameter	unit	value
cathode material	.	Cu
laser energy at the last viewport $E_{\text{laser}}$	$\mu\text{J}$	0.47
laser wavelength $\lambda_{\text{laser}}$	nm	266
laser photon beam energy $\hbar\omega$	eV	4.66
laser rms pulse length $\sigma_t$	ps	6.5
laser rms spotsize on cathode $\sigma_{\text{laser}}$	$\mu\text{m}$	330
single bunch charge $Q$	pC	0.6
pulsor gap voltage	kV	160
size of gap between cathode and anode	mm	4
gun gradient	MV/m	40
Schottky potential wall lowering $\phi_{\text{schottky}}$	eV	0.24
beam energy at gun exit $E$	keV	160
rms beam energy spread at gun exit $\sigma_{dE}$	eV	0.03
peak current $I_{\text{peak}}$	A	0.04
minimum rms beam size on YAG2 $\sigma_{x,y}$	$\mu\text{m}$	210
thermal emittance range from solenoid scan $\epsilon_{\text{th}}$	$\mu\text{m}$	0.2
work function from QE measurement $\phi$	eV	4.71
thermal emittance from QE measurement $\epsilon_{\text{th,QE}}$	$\mu\text{m}$	0.12

solenoids were installed in the diagnostic beamline. A dedicated emittance monitor with a movable pepperpot and a movable YAG screen (YAG2) was developed to measure the projected emittance in the space charge dominated region [5, 6]. The acquired beam image on a  $50 \mu\text{m}$  thick YAG2 screen is transferred to a digital CCD camera by an X-ray FELs

output-coupling mirror in a telescope [6]. The other  $50 \mu\text{m}$  thick YAG screen (YAG1) was installed to adjust the beam optics and to quickly check beam position. The optical resolution for the YAG1 screen is about 50 to  $100 \mu\text{m}$ , while the optical resolution for the YAG2 screen is about  $10 \mu\text{m}$ . Since the thermal emittance is normally a low value, YAG2 was used to measure a small beam size with a good resolution. Details of the beamline layout and machine parameters during the thermal emittance measurements are shown in Fig. 1 and summarized in Table 1.

## THERMAL EMITTANCE

Generally, there are five main contributions to the total projected emittance at the exit of a photo-emission gun, which can be summarized as

$$\epsilon_t = \sqrt{\epsilon_{\text{th}}^2 + \epsilon_{\text{lsc}}^2 + \epsilon_{\text{nsc}}^2 + \epsilon_{\text{rf}}^2 + \epsilon_{\text{optics}}^2}, \quad (1)$$

$$\epsilon_{\text{th}} \simeq \sigma_{\text{laser}} \sqrt{\frac{\hbar\omega - \phi + \phi_{\text{schottky}}}{3m_e c^2}}, \quad (2)$$

$$\phi_{\text{schottky}} \simeq 3.7947 \times 10^{-5} \sqrt{E(\text{V/m})} \text{ eV}, \quad (3)$$

$$\epsilon_{\text{lsc}} \propto \frac{Q}{(2\sigma_r + \sigma_z)E}, \quad (4)$$

$$\epsilon_{\text{nsc}} \propto \frac{FQ}{\sigma_r^2 \sigma_z}, \quad (5)$$

$$\epsilon_{\text{rf}} \propto f_{\text{rf}}^2 \sigma_r^2 \sigma_z^2 E, \quad (6)$$

$$\epsilon_{\text{optics}} \propto \frac{\sigma_\delta \sigma_r^2}{f_{\text{sol}}}, \quad (7)$$

where  $\epsilon_{\text{th}}$  is the thermal emittance on the cathode due to a non-zero kinetic energy of the emitted electrons,  $\epsilon_{\text{lsc}}$  and  $\epsilon_{\text{nsc}}$  are the contributions due to the linear and nonlinear space charge forces, respectively.  $\epsilon_{\text{rf}}$  is the contribution due to oscillating electromagnetic RF fields, and  $\epsilon_{\text{optics}}$  is the contribution of chromatic effects in the gun solenoid due to a non-zero energy spread [8–12]. Furthermore,  $\sigma_{\text{laser}}$  is the rms laser spotsize on the cathode for a round laser beam,  $\hbar\omega$  is the photon beam energy of the laser,  $\phi$  is the work function of the cathode,

$\phi_{\text{schottky}}$  is the lowering of the potential wall barrier due to the Schottky effect under an accelerating field  $E$ ,  $m_e c^2$  is the rest mass energy of an electron,  $\sigma_r$  is the rms beams size,  $\sigma_z$  is the rms bunch length,  $F$  is a form factor, which is zero for a 3D uniform ellipsoidal laser pulse,  $f_{\text{rf}}$  is the frequency of the oscillating RF fields in gun,  $\sigma_\delta$  is the relative rms energy spread, and  $f_{\text{sol}}$  is the focal length of the gun solenoid [8–12].

Normally, the emittance contribution due to the linear space charge force can be easily compensated by the main gun solenoid, while the emittance contribution due to the nonlinear space charge force can be eliminated with a special laser pulse shape such as the 3D uniform ellipsoidal pulse or with an extremely small single bunch charge [8]. Therefore the thermal emittance and the emittance due to the nonlinear space charge force define the minimum achievable slice emittance.

From Eq. (1) to Eq. (7), we can expect that  $\varepsilon_t$  can be reduced to  $\varepsilon_{\text{th}}$  if the other emittance contributions due to space charge forces, oscillating electromagnetic RF fields, and chromatic effects in the solenoid are nearly negligible. In particular,  $\varepsilon_t \simeq \varepsilon_{\text{th}}$  becomes valid if the following three conditions are satisfied simultaneously: Firstly, a single bunch charge  $Q$  should be small enough to eliminate contributions due to linear and nonlinear space charge forces [9, 10]. Secondly, the frequency of electromagnetic fields should be close to the DC level to remove the contribution due to electromagnetic RF fields [9, 10]. Thirdly, energy spread along a whole bunch should be negligible to avoid chromatic effects in the solenoid [8]. Generally, all three conditions can not be satisfied simultaneously in conventional RF guns. Recently, several laboratories with RF guns reported their measured thermal emittances with copper and  $\text{Cs}_2\text{Te}$  cathodes [13–15]. However, their measured thermal emittances were much higher than theoretically estimated values due to non-negligible RF field effects, space charge effects, chromatic effects, and resolution limitations in slit or pin-hole based emittance monitors. Their reported thermal emittances were higher than  $0.5 \mu\text{m}$ .

However, in our case, those three conditions can be satisfied simultaneously at the LEG test facility. During a beam acceleration period in the pulser, the electron bunch sees a constant DC voltage. Additionally, the rms electron bunch length of 6.5 ps is much shorter than the sinusoidal-like high voltage pulse length of 250 ns (FWHM). Therefore the rms energy spread along a single bunch is only about 0.08 eV at 500 keV, and contributions due to nonlinear electromagnetic RF fields and chromatic effects are negligible. To minimize emittance contributions due to linear and nonlinear space charge forces, we reduced the bunch charge down to about 0.6 pC by inserting laser-intensity attenuation filters in a laser transfer line. Furthermore, to solve the image noise and resolution limitation in the slit or pin-hole based emittance measurement system, we used the solenoid scan instead of the pepperpot method. In these experimental conditions, our measured total projected emittance  $\varepsilon_t$  should be close to the thermal emittance  $\varepsilon_{\text{th}}$ .

X-ray FELs

## EMITTANCE MEASUREMENTS

Generally, a solenoid can be considered as a focusing magnet with the normalized focusing strength  $k_{\text{sol}} = (eB_z/2cp)^2$  where  $e$  is the electric charge,  $B_z$  is the longitudinal solenoid field,  $c$  is the speed of light, and  $p$  is the momentum of electron [16]. If the effective length of the solenoid  $l_{\text{eff}}$  is much shorter than its focal length  $f_{\text{sol}} = 1/(k_{\text{sol}}l_{\text{eff}})$ , the solenoid can be considered as a thin focusing quadrupole [16]. Therefore the same principle of the well-known quadrupole scan can be applied to the solenoid scan [17].

After optimizing three solenoids (MSL10 to MSL30) to get a small round beam image on the YAG2 screen, we measured the beam size on the screen while scanning the solenoid current of MSL40. However, first of all, we had to remove the background noise in beam images during the solenoid scan to measure the beam size and thermal emittance with a high resolution. Typically, an intense dark current was emitted from copper electrodes as the gun gradient was higher than about 41 MV/m. Since the dark current is also a group of charged electrons with slightly different beam energies, its image on the YAG2 screen was also changed if focusing of the solenoid was changed during the scan. In this case, a fitting error in the beam size measurement occurred as shown in Fig. 3(top). To solve the background noise and the fitting error problem due to the dark current, 50 background images were taken by closing the shutter of the gun drive laser at the start of every

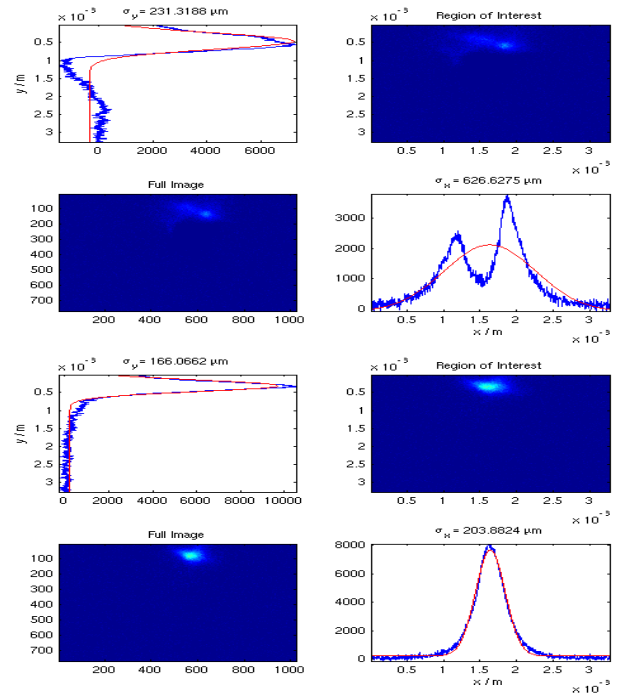


Figure 3: Impact of dark current on beamsize measurements; (top) a beam image with the dark current and background noises, (bottom) a pure beam image where the dark current and background noise were subtracted.

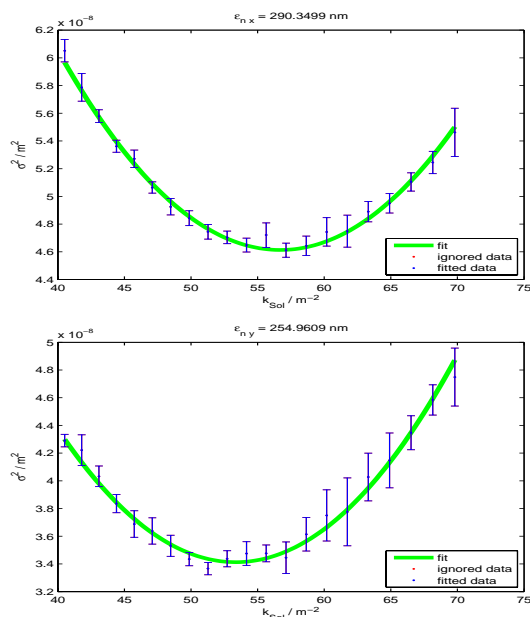


Figure 4: Typical thermal emittance measurement results with a diamond turned copper cathode at a gradient of 40 MV/m; the horizontal (top) and vertical (bottom) normalized thermal emittances. Here the vertical bars shown are the rms deviation of ten image measurements.

solenoid scan step. Then, an averaged background image from those 50 images was generated for the step. After this procedure, a normal beam image with the dark current was taken by opening the laser shutter. To obtain a pure clean beam image as shown in Fig. 3(bottom), we subtracted the averaged background image from a beam image with the dark current. At every scan step, we took ten beam images with the dark current, and repeated the same background subtraction procedure for those ten beam images to get a good statistics. Later, the statistics on beam size measurements was used to draw the vertical error-bars in the plot on the solenoid scan as shown in Fig. 4.

After acquiring images for all solenoid scan steps, the emittance can be deduced from the dependence of the square of the beamsizes  $\sigma_{x,y}^2$  on the solenoid focusing strength  $k_{sol}$  as shown in Fig. 4. With the same analysis method which we use for the well-known quadrupole scan, we can estimate the thermal emittance from a quadratic fitting between  $\sigma_{x,y}^2$  and  $k_{sol}$  [17]. Since  $l_{eff}$  of MSL40 is about 39.8 mm, the condition of the thin lens approximation was well satisfied in our scan range. In the case of one typical solenoid scan as shown in Fig. 4, the measured normalized horizontal thermal emittance is about  $0.29 \pm 0.01 \mu\text{m}$ , and its vertical thermal emittance is about  $0.26 \pm 0.01 \mu\text{m}$  for the rms laser spotsizes on the cathode of about  $330 \mu\text{m}$ . As summarized in Table 1, those measured emittances were routinely reproduced between  $0.18 \mu\text{m}$  to  $0.29 \mu\text{m}$  depending on machine operating conditions.

As shown in Fig. 5, we can also obtain the work function of the same copper cathode,  $\phi = 4.71 \text{ eV}$  from our X-ray FELs

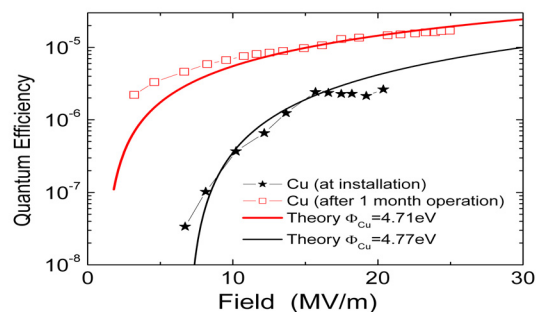


Figure 5: Quantum efficiency measurements with a copper cathode.

Quantum Efficiency (QE) measurement results [7, 11]. In this case, we can find the theoretically expected thermal emittance of the same copper cathode at 40 MV/m for  $\sigma_{laser} = 330 \mu\text{m}$  by using Eqs. (2) and (3), which is about  $0.12 \mu\text{m}$  as summarized in Table 1. This supports our belief that our measured range of  $0.18 \mu\text{m}$  to  $0.29 \mu\text{m}$  is really close to the theoretically estimated thermal emittance of about  $0.12 \mu\text{m}$ .

## SUMMARY

By removing emittance contributions due to RF fields, space charge forces, and chromatic effects, we have obtained a low thermal emittance of about  $0.2 \mu\text{m}$  with a copper cathode at the LEG test facility. Even if we scale our measured thermal emittance to that which one would expect with a higher gradient and a larger laser spotsizes, our scaled emittance is still much lower than previously reported values. From the QE measurements, we have cross-checked that our measured thermal emittance of about  $0.2 \mu\text{m}$  is closer to the theoretically estimated thermal emittance of about  $0.12 \mu\text{m}$  at 40 MV/m for  $\sigma_{laser} = 330 \mu\text{m}$ .

## REFERENCES

- [1] <http://fel.web.psi.ch>
- [2] Y. Kim *et al.*, in *Proc. EPAC2008*, Genoa, Italy.
- [3] Y. Kim *et al.*, in *Proc. LINAC2008*, Victoria, Canada.
- [4] M. Paraliiev *et al.*, in *Proc. IPMC2008*, Las Vegas, USA.
- [5] M. Pedrozzi *et al.*, in *Proc. EPAC2008*, Genoa, Italy.
- [6] V. Schlott *et al.*, in *Proc. DIPAC2007*, Venice, Italy.
- [7] F. Le Pimpec *et al.*, in these proceedings.
- [8] C. Limborg-Deprey, in *Proc. FEL2005*, Palo Alto, USA.
- [9] C. Travier *et al.*, *Nucl. Instr. and Meth. A* **340**, 26 (1994).
- [10] K.-J. Kim, *Nucl. Instr. and Meth. A* **275**, 201 (1989).
- [11] D. H. Dowell *et al.*, *PRST Accel. Beams* **9**, 063502 (2006).
- [12] K. L. Jensen *et al.*, *J. Appl. Phys.* **102**, 074902 (2007).
- [13] W. Graves *et al.*, in *Proc. PAC2001*, Chicago, USA.
- [14] J. F. Schmerge *et al.*, in *Proc. FEL2004*, Trieste, Italy.
- [15] S. Lederer *et al.*, in *Proc. FEL2007*, Novosibirsk, Russia.
- [16] H. Wiedemann, *Particle Accelerator Physics II*, 1993.
- [17] S.G. Anderson *et al.*, *PRST Accel. Beams* **5**, 014201 (2002).